ELSEVIER

Nuclear Engineering and Design 146 (1994) 133–146

Nuclear Engineering and Design

On the fundamental microinteractions that support the propagation of steam explosions

W.W. Yuen *, X. Chen *, T.G. Theofanous

University of California, Santa Barbara, Center for Risk Studies and Safety, Department of Chemical and Nuclear Engineering, Santa Barbara, CA 93106, USA

Abstract

This paper makes available the first experimental data on the fragmentation kinetics of hot liquid drops in another liquid (coolant) under the influence of sustained pressure pulses. We observe the effect of "thermal" on "hydrodynamic" fragmentation and micromixing mechanisms, as deduced by the rates and morphology of the resulting particle "cloud". We show how propagation can be quantified within the framework of a numerical model, and on this basis some interesting interpretations of an experimentally-observed triggered "detonation" in the KROTOS facility (in ISPRA) are offered.

1. Introduction

It is known that under certain conditions "hot" liquid drops can violently interact ("explode") after coming in contact with a surrounding "cold" and volatile liquid (the "coolant"). These thermal interactions are the consequence of rapid and fine fragmentation (of the drop) and the accompanying mixing with the surrounding coolant. Such interactions are known to be initiated by the contact of the two liquids; such contact can be observed either spontaneously (for appropriate combinations of temperatures) or it can be caused by forcing the collapse of the intervening vapor blanket, as for example, by a sharp pressure pulse. It is also known that droplet fragmentation can result from purely hydrodynamic causes (i.e. in isothermal systems) in an induced rapid acceleration environment, as the one that accompanies a large pressure wave. In the detonation wave of a steam explosion clearly both mechanisms are present, yet their relative role, and hence the actual kinetics that control the various stages of escalation from the initiating trigger event to a "full-strength" detonation, remain to be reconciled.

More specifically, while the very initial stages of a spontaneously triggered explosion will be dominated by thermally-induced fragmentation, and while at the other extreme of a fully developed detonation into the supercritical pressure region only hydrodynamic breakup is relevant, nothing is known about the intermediate, escalation, regime. *This regime is crucial in that it determines whether the premixture conditions can support an escalation into a highly developed detonation, and perhaps more importantly, whether this escalation is possible within the physical constraints of the practical system under investigation.*

* Also with the Department of Mechanical and Environment Engineering.

SSDI 0029-5493(93)E0225-9

This then is the main theme of this work, with some more specific considerations including: the details of micromixing environment around each drop as it fragments, the dynamic aspects of the pressure and velocity fields behind the shock front (especially in the so-called reaction zone), and the fundamentally non-one-dimensional character of the process. Our experimental approach is based on the detailed observation of droplets forced to interact with the coolant in a simulated steam explosion environment – especially with regard to *sustained* pressure waves that characterize the reaction zone. This is accomplished in a hydrodynamic shock tube. All analytical interpretations are carried out with our computer code, ESPROSE, already documented by Medhekar et al. [1,2].

Previous related work can be briefly summarized as follows.

1.1. Thermally-induced fragmentation

Most of the work in this area has been aimed to delineate and interpret the so-called temperature interaction zone. No fragmentation rate data exist, but inferences on fragmentation (and interaction) rates have been made from comparisons of calculations with Nelson's [3] data on the growth and collapse cycles of vapor bubbles from triggered single-drop melt-water interactions. Such interpretations have been offered by Kim and Corradini [4] and by Inoue et al. [5] among others. In particular, the Kim–Corradini model is intended to be predictive; in it the fragmentation time is obtained from the penetration of the drop by liquid coolant jets arising from the "spikes" of Taylor waves at the interface upon collapse and rebound of the vapor blanket. In a simple interpretation [16] of this model the jet velocity is obtained from

$$U_j = \left\{ \frac{\Delta P}{\rho_c (1 + \rho_d/\rho_c)^{1/2}} \right\}^{1/2}, \tag{1}$$

which yields a fragmentation time t_b of

$$R_d/U_j < t_b < D_d/U_j. \tag{2}$$

In the above, ΔP is the pressure rise across the shock front. Note that this model makes no distinction for the duration of the pressure pulse or of the droplet temperature, and it does not explain how these microscopic jets can survive the intense heating environment, but rather penetrate the droplet all the way through. For example, for a corium melt drop 10 mm in diameter, and a shock pressure rise of 200 bar, the above yields a fragmentation time of 50 to 100 μs. Note that this is short compared to the residence time in the reaction zone, and too long regarding the microjet's potential response to the intense heating.

1.2. Hydrodynamically-induced fragmentation

Experimental work in this area, for the relevant liquid–liquid system, is scarce and not well documented; worse, it appears to be contradictory. On the one hand Baines et al. [6] and Kim et al. [7] working with mercury and gallium drops in water have reported (visual determination) fragmentation times consistent with old results obtained in gas–liquid systems; namely, the boundary layer stripping mechanisms and a dimensionless fragmentation time, t_b^*, of

$$t_b^* \equiv \frac{t_b U_r}{D_d} \left(\frac{\rho_c}{\rho_d} \right)^{1/2} \sim 4 \text{ to } 5. \tag{3}$$

On the other hand, Theofanous, Saito and Efthimiadis [8], using flash X-ray diagnostics reported, for a mercury–water system, significantly lower breakup times. These results were correlated in terms of a $Bo^{1/4}$ dependence, motivated by a Taylor instability mechanism, as

$$t_b^* = 10.3\ Bo_o^{-1/4}. \tag{4}$$

For example, for a Bond number of 10^4 this yields a dimensionless breakup time of ~ 1, or four to five times faster than boundary layer stripping. For a Bond number of 10^3 the result is ~ 2 and still more than a factor of 2 faster. Both the X-ray photos and the quantitative analysis of them has been documented by Theofanous et al. [9].

1.3. Fragmentation in detonation models

Not surprisingly, the formulation of fragmentation in detonation modelling has been widely varied. To start with, the formulation in the original, steady-state, detonation model of Board and Hall [10] made use of Eq. (4), with a coefficient of 22, known at the time from experiments with gas–liquid systems. Modern transient detonation models have also made use of hydrodynamic fragmentation; Thyagaraja and Fletcher [11] used a uniform fragmentation rate based on Eq. (3), but, for unknown reasons, with the constant set equal to 1; Medhekar et al. [1,2] used the Reinecke–Waldman fragmentation rate correlation [12] (developed also from gas–liquid work) with a dimensionless fragmentation time of 1 (motivated from Eq. (4)). It should be noted that all these (gas–liquid) data were obtained with steady flow conditions (by imposing an instantaneous acceleration and thus a fixed free-stream velocity behind the shock) while for liquid–liquid systems the relative velocity changes during the fragmentation time is very significant. In a detonation calculation this is further aggravated by the highly variable pressure and velocity field histories behind an escalating shock front. Finally, besides the fragmentation kinetics, another equally important aspect in detonation modelling is to properly reflect the micromixing between the finely fragmented debris and the coolant available to mix in the immediate proximity. This is particularly important in fuel–dilute premixtures (as is commonly the case) and also in interpreting experiments that may not be truly one-dimensional. As experienced by Bürger et al., [13] one-dimensional simulations lead to considerable inconsistencies – with the exception of ESPROSE, all other published detonation models are restricted to one dimension.

The presentation in this paper is made in three parts. The first is concerned with the recasting of Eq. (4) in differential form; that is, expressing the fragmentation rate in terms of the instantaneous Bond number. This is done with the help of ESPROSE made to simulate the single-drop response as observed in the shock-tube experiments that formed the basis for Eq. (4). In the second part we present new experimental data, obtained in the same shock-tube facility but with molten tin drops superheated by different amounts and subjected to pressure waves of various magnitudes, such as to span the potential range of thermal vs. hydrodynamically controlled mechanisms. A preliminary interpretation of these data (hydrodynamic vs. thermal fragmentation mechanisms) is also provided with the help of ESPROSE and the instantaneous Bond number formulation derived in the first part. Finally, in the third part these fragmentation kinetics results are supplemented with a non-equilibrium treatment introduced in ESPROSE to "simulate" and discuss a "detonation" observed in the KROTOS facility at the European Joint Research Center in ISPRA (Italy). This example also illustrates the importance of two-dimensionality even for apparently one-dimensional situations.

2. The instantaneous Bond number formulation

The operation of the hydrodynamic shock tube (the SIGMA facility) was simulated with ESPROSE by introducing a small enough mercury mass in one computational shell to correspond to the one drop used in the experiments. The facility and experimental technique have been described previously [14]. Briefly, a prescored diaphragm is ruptured, to suddenly release the pressure from the 1.2 m long driver section into the water-filled 3 m long expansion section. The tube is designed for pressures up to 1000 bar. In the particular experiments considered here (isothermal at room temperature) the mercury drops were initially stationary (resting on a thin teflon piece) and the fragmentation states were determined from flash X-ray radiograph obtained for different delay times after the arrival of the shock. The fragmentated mass on these X-ray films was determined [9] from the mass found in the "particle cloud" by quantitative image analysis. (This method is demonstrated for tin drops in the next section). The driver pressures in this set of experiments were set at 200, 333 or 466 bar. We could match the data well with an instantaneous fragmenta-

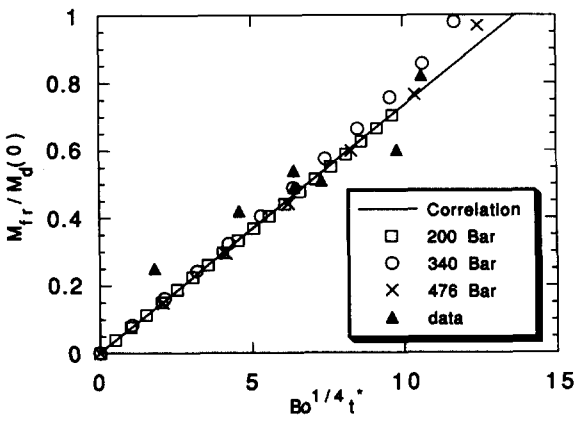

Fig. 1. Computed fragmented mass (○, □, ×) in comparison to experimental data in the mercury/water system (isothermal). The solid line is $13.7\, t_b Bo_o^{1/4}$.

tion rate given by

$$\frac{dM_d}{dt} = -\frac{\pi D_d^2(t)\,|U_d(t) - U_c(t)|}{6t_b^*}(\rho_c\rho_d)^{1/2} \tag{5}$$

with a dimensionless breakup time given in terms of the instantaneous Bond number by

$$t_b^* = 13.7\ Bo_i^{-1/4}. \tag{6}$$

Note that in the implementation of Eqs. (5) and (6), all fluid properties and flow velocities are evaluated at their instantaneous values. The results are shown against the experimental data in Fig. 1.

The detailed results from the 200 bar simulation are summarized in Fig. 2. In particular, we can observe the changes in relative velocity, particle diameter, and the resulting variation of the Bond number. The evolution of the debris volume fraction distributions is also shown – this is of significance in gaining some perspective on local mixing obtained and resulting pressure feedback effects responsible for sustaining a propagation. The computed liquid and droplet velocities are in good agreement with the data. The computed shock front exhibits minimal numerical diffusion, and its speed is also in excellent agreement with the data. The node size in

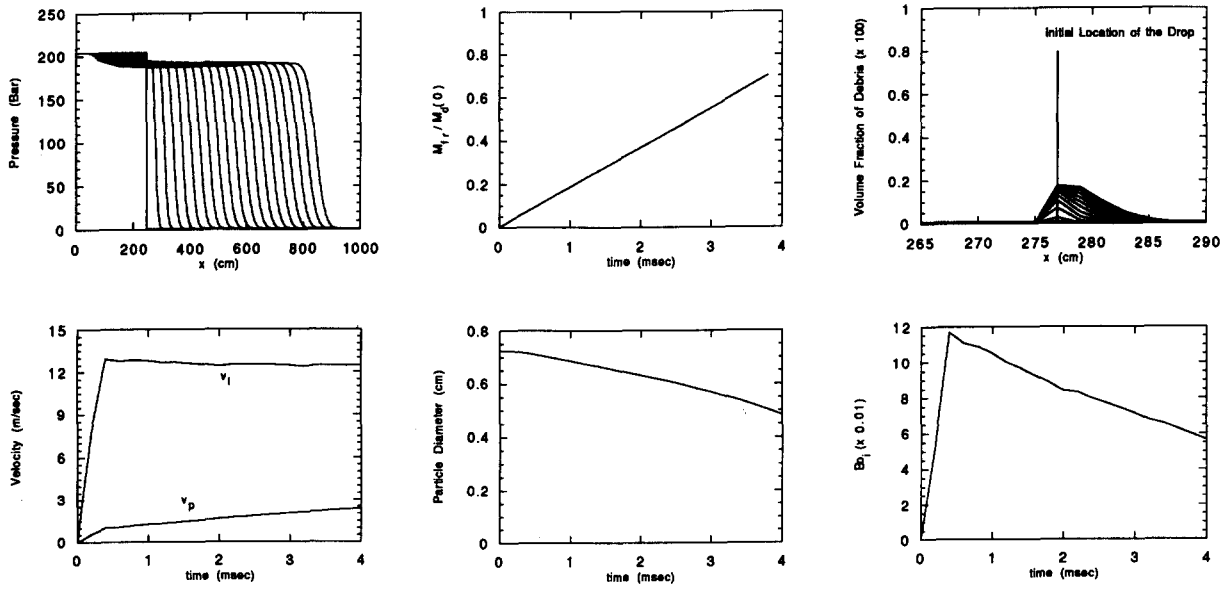

Fig. 2. Detailed results from an ESPROSE simulation of a mercury drop subjected to a 200 bar shock in water. The distance x is along the length of the shock tube starting at the top of the driver section. The position of the diaphragm is at $x = 250$ cm (in this simulation a longer tube, than in the experimental one, was chosen to allow a longer evolution of the transient before reflected waves arrive back at the drop). The pressure front is given in time increments of 0.2 ms. In the debris volume fraction plot, the time increment is 0.4 ms. In the time plots, the origin is at the shock arrival time to the droplet position.

this computation was 1 cm and the time step, 0.01 ms.

Similar calculations were carried out for the boundary layer stripping and the Reinecke–Waldman correlations discussed above. In these calculations the correlations were used in their differentiated form and with the instantaneous flow/drop parameters during the transient. The results for different combinations of pressures and fragmentation time are collected in Fig. 3. We observe that

(a) the Reinecke–Waldman formulation cannot be made to agree for any choice of t_b^*, and
(b) although for particular conditions there are particular choices of t_b^* to produce reasonable agreement, no single choice can cover the whole range of the conditions of interest.

Further testing of the presently proposed formulation under more extreme conditions of Bond number variation during the transient (for example, by shaping the pressure pulse – this can be done by inserts in the driver section) is deemed desirable.

3. Fragmentation of molten tin drops

For these experiments the SIGMA facility was equipped with a melt generator, a device that could produce and release a single (occasionally

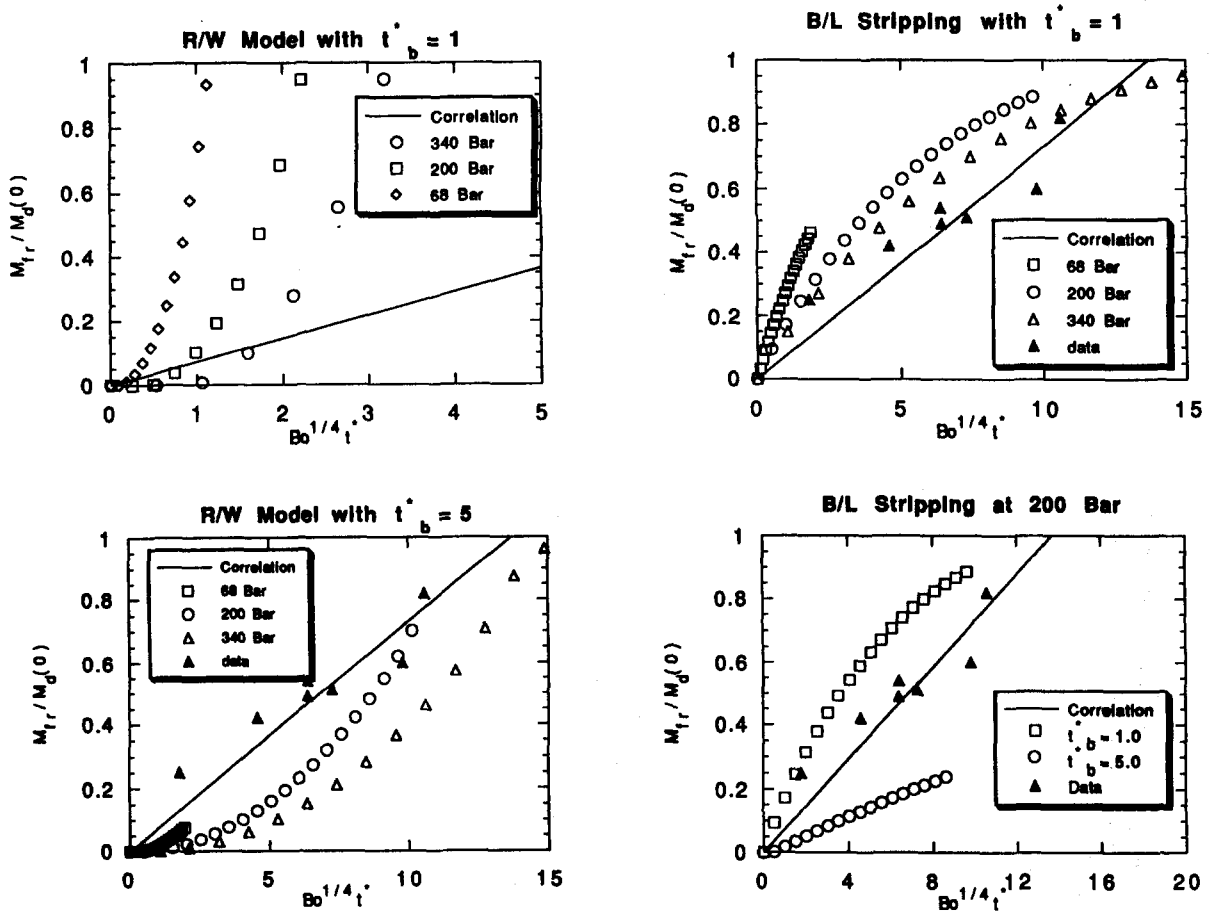

Fig. 3. Comparison of the Boundary Layer Stripping and the Reinecke–Waldman correlations (for various choices of t_b^*) with the experimental data in a mercury/water system.

split into two equal parts) drop of molten tin at required temperatures of up to 1000°C (at this time). Data were obtained at low (360°C), intermediate (670°C), and high (1000°C) temperatures, and at two shock (pressure) levels, 66 and 200 bar. The drop temperature (quoted at the time of shock impact) was reproducible with ±20°C. In all experiments the drop mass was fixed at 1 g and the water pressure and temperature at 1 bar and 85°C (to prevent spontaneous interactions), respectively. The shock was timed to hit the drop while it is within view of the shock tube window. This timing could be adjusted so that the drop remained in view for times up to 2 ms following impact. In the present configuration, the pressure/flow conditions of the water in the viscinity of the droplet remain unchanged for up to 2.5 milliseconds, at which time the reflected shock travelling back from the bottom of the tube arrives. As noted already, however, by appropriate modifications in the driver section a wide range of pressure pulse shapes can be obtained. Also, a

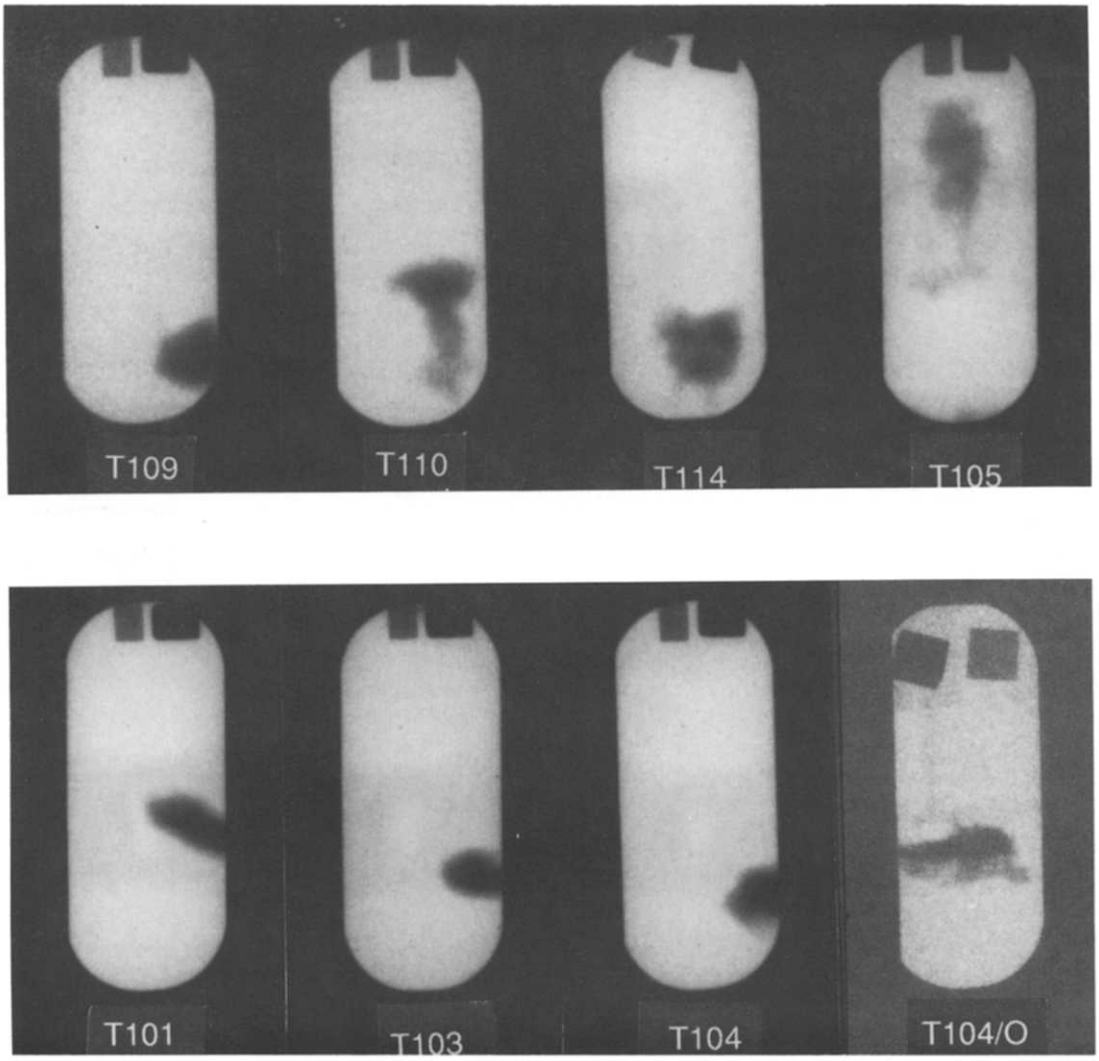

Fig. 4. X-ray snapshots from the runs with 66 bar shocks. Tin temperatures of 1000°C and 670°C for the top and bottom rows, respectively. Times (in ms) following shock arrival: T109–1, T110–1.5, T114–1.5, T105–2, T101–0.5, T103–1, T104–2, T104/0–2.

two-phase flow environment around the drop can be generated by means of steam injection at the bottom of the tube. Such experiments are currently in progress. Also, the initial pressure (in the expansion section) can be varied – such experiments are now planned for the future.

As in the mercury/water experiments discussed above, data were obtained from single flash X-ray exposures at different times along the fragmentation process. Since all conditions are highly reproducible, these data provide the timewise evolution of a "representative" drop as well. In these older experiments, the unfragmented portion of the drop could not be adequately penetrated, even with hard X-rays (30 kV in the Hewlett-Packard generator). Thus, only the fragmented mass (debris cloud) could be quantified. In the present experiments with tin, the whole

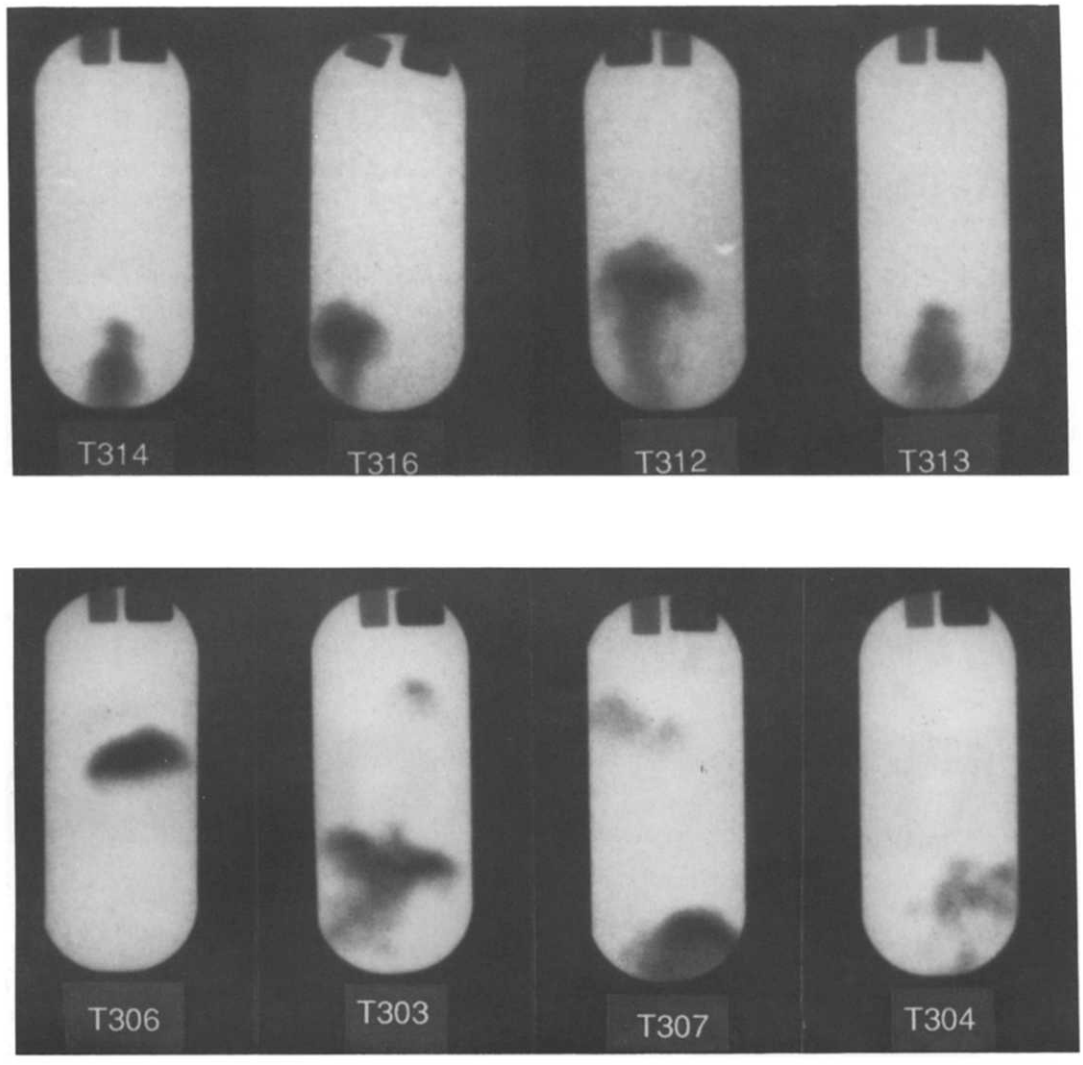

Fig. 5. X-ray snapshots from the runs with 200 bar shocks. Tin temperatures of 1000°C and 670°C for the top and bottom rows, respectively. Times (in ms) following shock arrival: T314–0.75, T316–0.85, T312–1, T313–1.5, T306–0.75, T303–1, T307–1.5, T304–2.

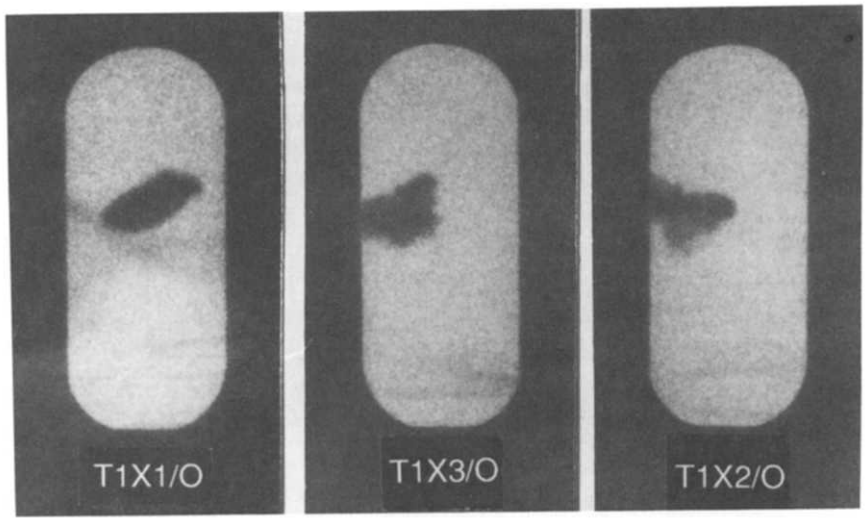

Fig. 6. X-ray snapshots from the low temperature (360°C) runs with 66 bar shocks. Times (in ms) following shock arrival: T1X1/0–0.25, T1X2/0–1.5, T1X3/0–2.

drop can be penetrated, even with soft X-rays (24 kV, using the soft X-ray tube), and the whole image, including the unfragmented part, could be quantified. The procedure involved the use of a calibration curve obtained from exposing a tin stepwedge and two (later three) "witness" pieces to allow for variability in the exposure (small) and film development (quite significant). The X-ray image was digitized by a scanner creating a two-dimensional array of light intensities. These data were then processed by the computer using the calibration curve (with appropriate normalizations, based on the witness pieces) to obtain a two-dimensional array representing the spatial distribution of tin mass. A test of the accuracy of the procedure is the extent to which these calcu-

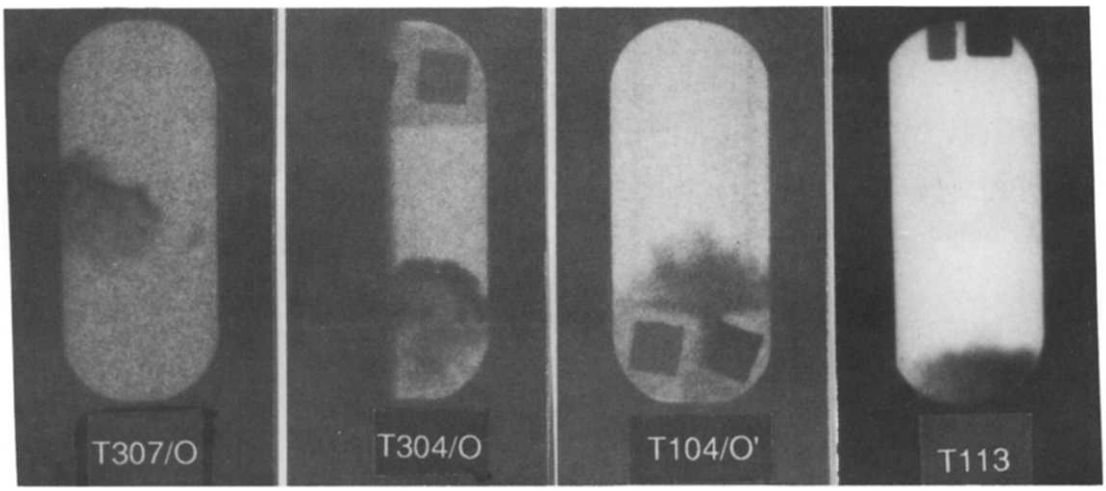

Fig. 7. Snapshots from miscellaneous runs. Shock pressures of 66 and 200 bar for the 100- and 300-series, respectively. Tin temperature 1000°C for T113 and 670°C for all others. Times (in ms) following shock arrival: T307/0–1.5, T304/0–2, T104/0'–2, T113–1.5.

lated masses add up to the known total drop mass (1 g, or 0.5 g for the case of split drops). From the results obtained so far (discussed below) this test was met beyond our expectations. Because of the non-linearities involved, visual inspection of such films can be quite misleading, and such quantitative results are essential to understanding the fragmentation process.

Additional information about the extent and intensity of the interaction, in an overall sense, is available from the debris which is collected with an especially constructed plastic "pan" located some 10 cm below the interacting drop. These data have not been analyzed in detail yet, but typically they are composed of two groups of masses – one highly fragmented at micron-size round spheres and the other highly porous, but macroscopic in dimension, particles. In the 1000°C runs, for which these data are available, this macroscopically fragmented mass amounted to 50% and 40% of the drop mass for the 66 and 200 bar runs, respectively. Thus, as a first indirect measure it appears that at 1000°C about one-half of the drop is finely fragmented, with a bias for more fragmentation at the higher shock pressures.

All the X-ray results obtained so far can be found in Figures 4 through 7. The 100-series runs in Fig. 4 were obtained with shock pressures of 66 bar (1000 psi), while the 300-series results obtained with shock pressures of 200 bar (3000 psi) are in Fig. 5. In these figures the top line is for tin drop temperatures of 1000°C while the bottom line for 670°C. In Figs. 6 and 7 we have collected certain "older" experimental data obtained during the development of the experimental techniques. As such the conditions for these "old" data are not very reliable, but they are included here because of certain interesting features in the fragmentation morphology they exhibit.

Before discussing these data, it is useful to have in mind Fig. 8, which shows in real time the expected fragmentation of a tin drop according to the hydrodynamic fragmentation model (the instantaneous Bond number formulation discussed in the previous section). Also, it is useful to consider the digital X-ray "reconstructions" (i.e., mass distribution) for runs T109, T312 and T313 as shown in Fig. 9. The total mass computed for T109 and T312 was 0.98 g and 0.89 g, respectively, while for runs T113, which was apparently a split drop, the mass adds up to 0.49 g.

The following observations can now be made:

(a) At low tin temperatures (360°C), even at 2 ms, the fragmentation observed under a 66 bar shock is negligible. This is consistent with Fig. 8.

(b) At intermediate tin temperatures (670°C) fragmentation is again negligible (up to 2 ms) under a 66 bar shock, but a catastrophic breakup is seen to occur at just before 1 ms under a 200 bar shock. This is clearly thermally driven as it is far faster than that expected from the hydrodynamic mechanism (see Fig. 8) and is also suggested by the morphology (see Fig. 5). As seen by the result of T304, by 2 ms "there is nothing left."

(c) At high tin temperatures (1000°C) thermally driven fragmentation seems to set in already at 66 bar (it is essentially complete by ~ 1.5 ms) but, again, it is faster at 200 bar (see T312 in Figs. 5 and 9).

(d) In both T101 and T109, both taken at 1 ms, it appears that something is already beginning at the interface – see also T109 in Fig. 9. However, it is also clear that there is a significant delay time before thermal fragmentation can be seen to be clearly in progress. This

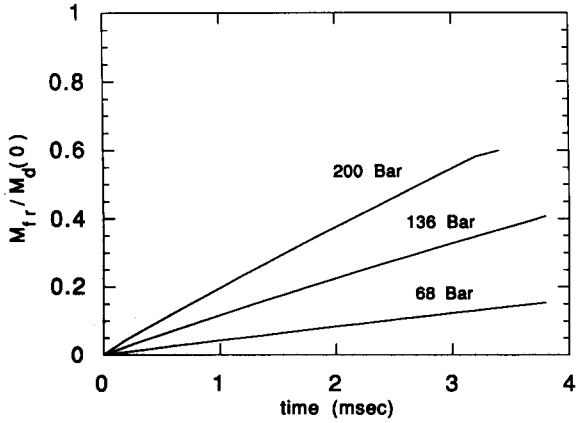

Fig. 8. Hydrodynamic fragmentation in tin/water system. ESPROSE with the instantaneous Bond number formulation.

delay time seems to be decreasing as shock pressure and/or tin temperature increase.

(e) Finally, attention is directed to the interesting *and varying* morphologies seen in tests T114 and T303 (seeming to have caught the very early stages of a fully developing event) and in tests T105 and T304 (showing the final, highly dispersed stage). Also very interesting is test T104/0′ showing an upward-directed fragmentation event with quite a lot of detail on the interfacial structure.

It is clear from these results that neither Eq. (1) nor Eq. (6) capture the essential physics involved in the thermal or combined thermal-hydrodynamic regimes of fragmentation. Moreover, the various interdependencies on shock pressures and melt temperatures seem to be rather complex. Based on this, it can be expected that even the pressure pulse duration (in fact shape) will play an important role in the process. Clearly, more such data are necessary if this key ingredient to predicting the escalation and potential intensity of detonations in explosive premixtures is to be adequately pinned down.

4. Discussion of an experimentally observed detonation

In this section we apply ESPROSE to perhaps the only reasonably characterized detonation observed experimentally. It was run in the KROTOS facility in ISPRA [15]. In it, 7 kg of molten tin at 1075°C was dropped (in the form of a jet) into a vertical pipe (9.5 cm in diameter, 1.09 m long) full of 85°C water. When the first melt arrived at the bottom, an explosion was triggered by rupturing a diaphragm and thus releasing 15

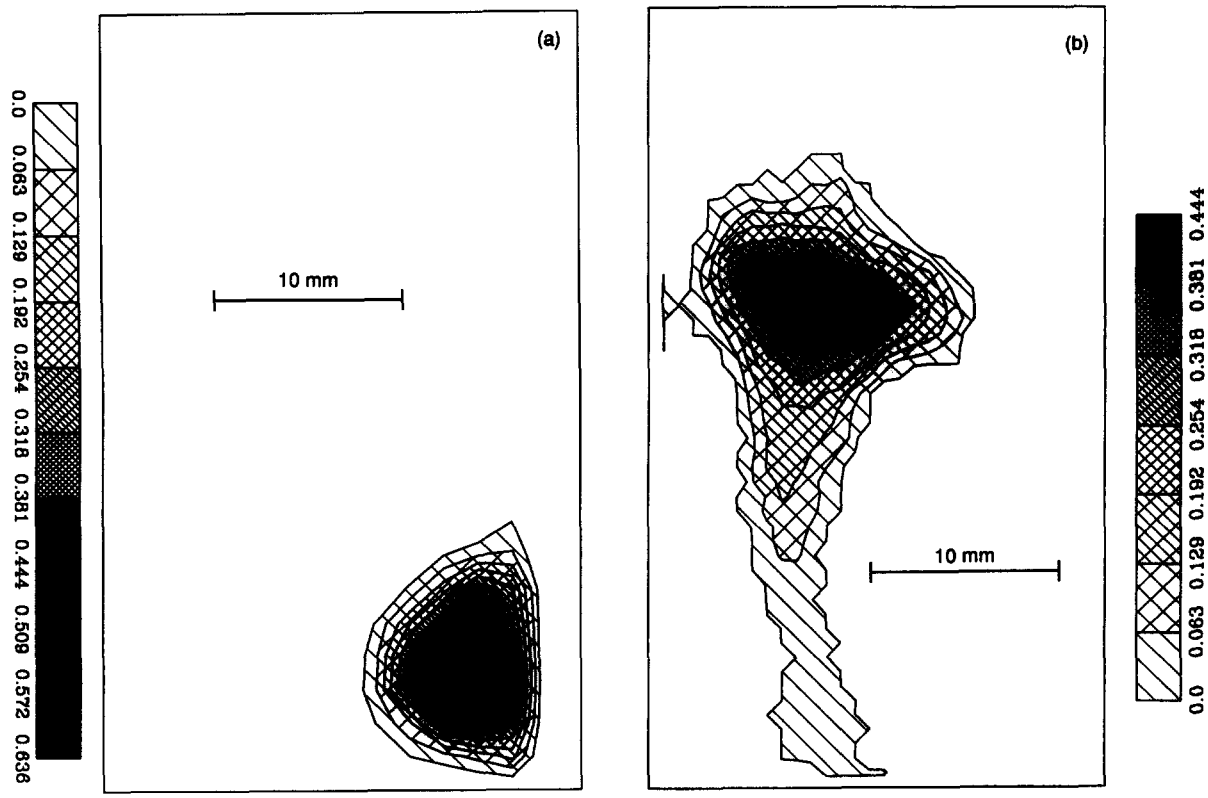

Fig. 9. Digital reproductions of the X-ray films for runs T109 (above), T312 (top next column) and T313 (bottom next column). The numbers in the shade-scale are in cm. Note that the diameter of a 1 g spherical tin drop is 0.66 cm.

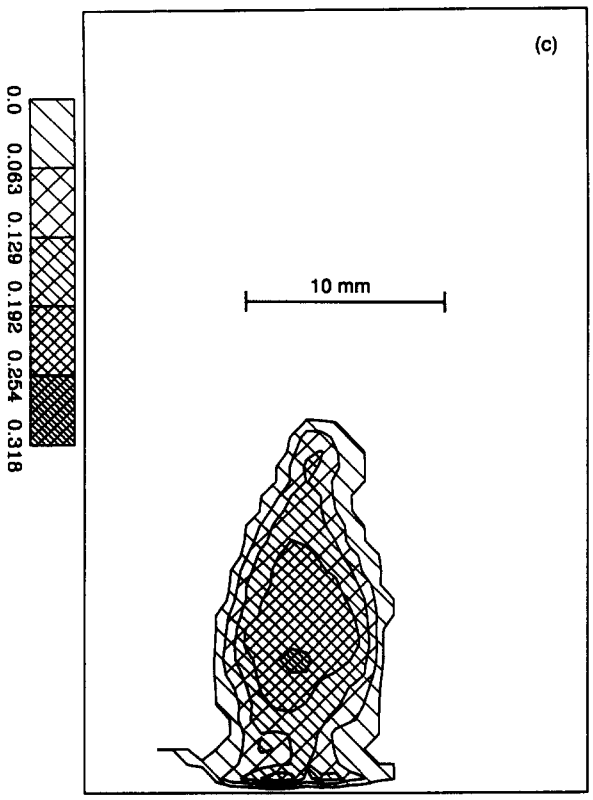

Fig. 9 (continued).

cc of compressed nitrogen at 120 bar into the lower end of the tube. The explosion was recorded by pressure transducers found all along the tube. We used the term "reasonably" rather than "well" characterized, above, because an important quantity, the steam volume fraction along the tube during the premixing, was not measured. However, this can roughly be estimated from the shock wave trajectories measured experimentally. [15] Such a void fraction distribution is used in the present calculations, but with the void concentrated in the inner radial node. The molten tin $\sim 1\ \ell$ t was distributed evenly along the center of the tube.

The object of this numerical exercise is to show the importance of local non-equilibrium (within the coolant), of fragmentation kinetics, and of their interplay in the development of triggered explosions. Thus, the ESPROSE code (model fully specified in Medhekar et al. [1,2]) was used with the following changes.

(a) In place of the original phase change model used to drive the system to equilibrium through a relaxation time constant, we put in a phase change rate obtained from the difference in heat flux transported through each phase to the interface. The constitutive laws for these fluxes are as in the original model.

(b) The fragmentation kinetics were based on the hydrodynamic fragmentation correlation described in this paper (based on the instantaneous Bond number). This choice was made because, as shown above, a formulation for thermally-driven fragmentation under the conditions of interest is still lacking, and also because of the particular purpose of the illustration intended here.

A difficulty with one-dimensional models, as encountered by Bürger et al. [15] in an attempt to interpret this same KROTOS test, is that even in apparently 1-D geometries (as the present one) they are forced to mix the debris with too much water – thus "quenching" the escalation. On the other hand, by using less water (in each axial node) the actual compressibility of the system is distorted. In the present calculation, this can be partly overcome by using two radial nodes (the inner one of radius 2.375 cm).

Even with the above description, some of the phase change dynamics early on cannot be captured, as very small quantities of fragmenting fuel contact very small quantities of the adjacent water thus leading to very high local non-equilibrium in the coolant/debris field. To generate a perspective on this, several calculations were run with different *specified* fractions of the fragmenting debris energy given directly to vapor production – the rest of the energy is supplied to the coolant in the node to which the debris is released. For this fraction, set at 10%, a very strong escalation was calculated in less than 0.25 ms. Similarly, for this fraction at 5%, the calculated explosion was much stronger than observed experimentally in just 0.5 ms. A fraction of only 2.5% was necessary to match the observed propagation. In this case, the total fragmented mass in the 3.75 milliseconds of the calculation was only

354 g (out of a total of 6.5 kg), certainly a very weak explosion. The total mass used in the direct vaporization process was only 8.85 g. With no direct vaporization, the propagation fizzled out. This calculation is contrasted to the one that produced agreement with the data in Fig. 10. The comparison with the measured pressure traces in KROTOS is shown in Fig. 11.

Several points can now be made.

(a) The KROTOS test discussed involved a very mild thermal interaction; however, it was adequate to maintain the imposed trigger pulse.

(b) Unless the constitutive law used for condensation in this calculation is very inaccurate, it appears that only slight thermal interactions are needed to maintain the pulse in strongly triggered experiments. This raises the question of what is the relationship to a full detonation. Regarding the adequacy of the condensation laws, the possibility of shattering the gas/liquid interface and its effect on heat transfer remains to be examined.

(c) The issue of local micromixing and vapor production/condensation in the pressure field within the "reaction" zone needs further study, in conjunction with the fragmentation kinetics. Toward this purpose, future studies besides X-ray diagnostics will employ direct visualization.

5. Concluding remarks

This study makes available the first experimental data on exploding drops in an environment that simulates that of a propagating steam explosion. It also shows that fragmentation kinetics, and the micromixing behavior with the surrounding coolant, can be quantitatively derived by an X-ray imaging technique. The results show very interesting interplay(s) between thermal and hydrodynamic-in-origin fragmentation mechanisms. However, additional data are required before the necessary clues for theoretical developments can be discerned.

Further examination of hydrodynamic fragmentation kinetics supports the quantification proposed earlier by Theofanous et al. [8]. Using this correlation, and a non-equilibrium phase change treatment in a 2-D simulation of a KROTOS test by ESPROSE, we conclude that it de-

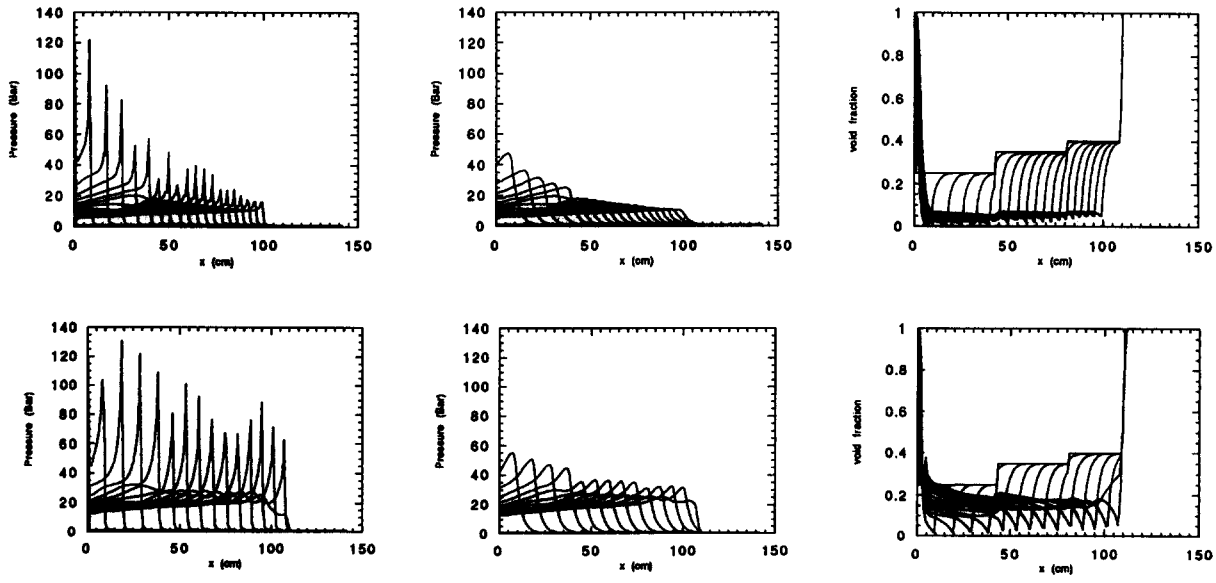

Fig. 10. ESPROSE simulations of the KROTOS test with (bottom) and without (top) direct vaporization from the debris–coolant interaction. The first and second figures in each row are for the inner and outer radial nodes, respectively. Print interval 0.25 ms. The third figures in each row show the void fraction in the inner radial node.

picts a barely sustainable propagation (involving very small quantities of melt). Suggestions for further investigation of local non-equilibrium phenomena in conjunction with fragmentation kinetics in simulated steam explosion "reaction" zones are made.

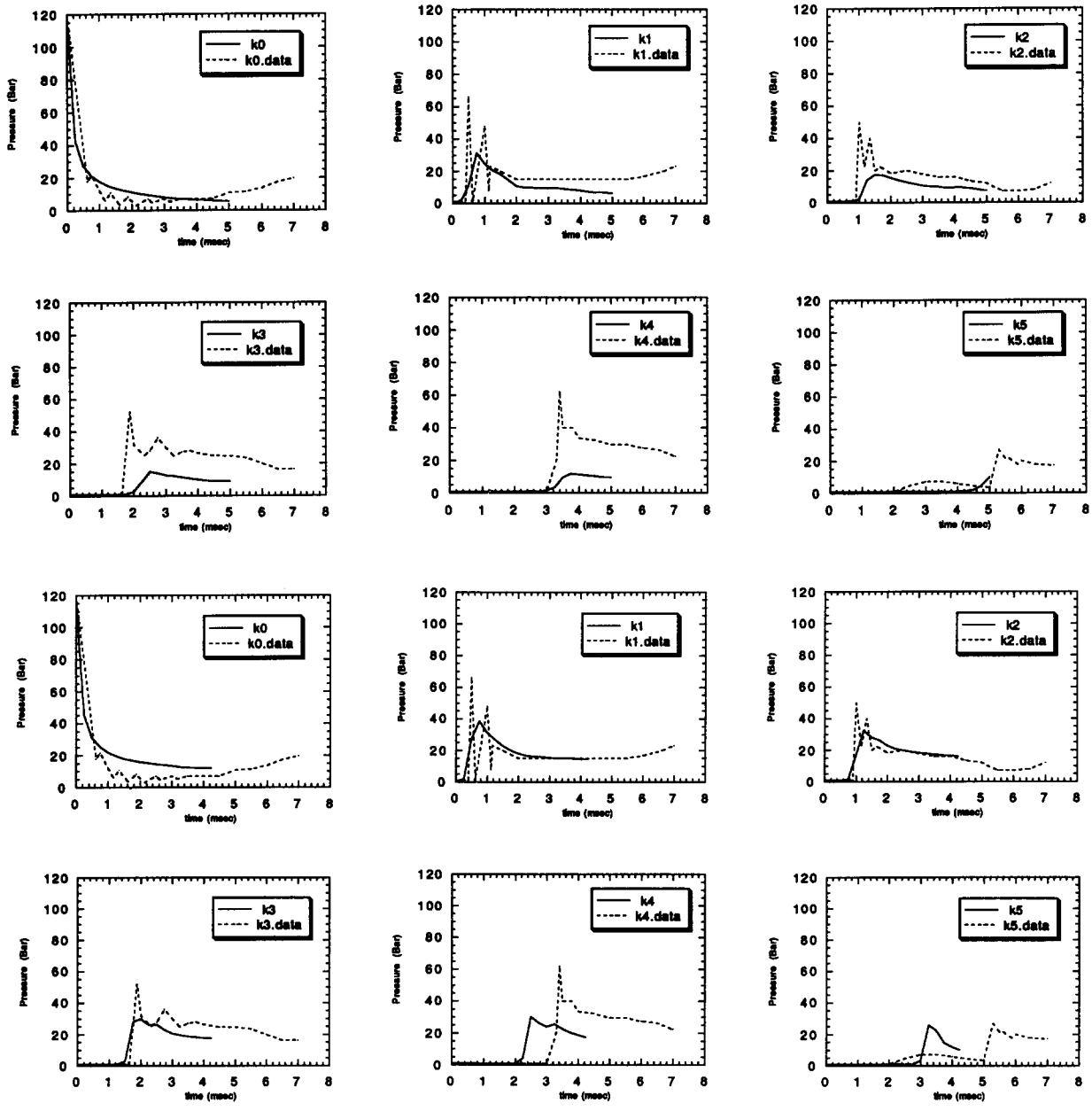

Fig. 11. Comparison of the pressure traces taken in the KROTOS test with ESPROSE results (outer radial cell). Top two rows "without" and bottom two rows "with" direct vaporization (corresponding to the heat from 2.5% of the fragmenting debris).

6. Acknowledgments

This work was performed for the U.S. NRC under contract 04-89-082. Dr. S. Medhekar and Mr. R. Buckles helped with the early development of the melt generator and related experimental technique.

7. Nomenclature

Bo $= 3/16[C_D \rho_c D_d (U_c - U_d)^2/\sigma]$,
C_D drag coefficient,
D diameter,
g density,
M mass,
R radius,
t^* dimensionless time,
t_b time required for breakup,
t_b^* dimensionless breakup time, and
U velocity.

7.1. Greek

ΔP pressure rise across shock front,
ρ density,
σ surface tension.

7.2. Subscripts

j coolant microjet,
c continuous phase, or coolant,
d dispersed phase, or droplet,
fr fragmented,
o initial value just after passage of shock,
r droplet-to-coolant relative value.

8. References

[1] S. Medhekar, M. Abolfadl and T.G. Theofanous, Triggering and propagation of steam explosions, Nucl. Engrg. Des. 126 (1991) 41–49.
[2] S. Medhekar, W.H. Amarasooriya and T.G. Theofanous, Integrated analysis of steam explosions, Proc. Fourth International Topical Meeting on Nuclear Reactor Thermal-Hydraulics, Karlsruhe, FRG, Oct. 10–13, 1989, Vol. 1, pp. 319–326.
[3] L.S. Nelson and P.M. Duda, Steam explosion experiments with single drops of iron oxide melted with a CO_2 laser, NUREG/CR-2295, U.S. Nuclear Regulatory Commission (September 1981).
[4] H.J. Kim, and M.L. Corradini, Modelling of small scale single droplet fuel–coolant interactions, Nucl. Sci. Engrg. 98 (1988).
[5] A. Inoue, M. Aritomi and Y. Tomita, An analytical model on vapor explosion of a high temperature molten metal droplet with water induced by a pressure pulse, Proc. Fourth International Topical Meeting on Nuclear Reactor Thermal-Hydraulics, Karlsruhe, FRG, Oct. 10–13, 1989, Vol. 1, pp. 274–281.
[6] M. Baines and N.E. Buttery, Differential velocity fragmentation in liquid–liquid system, Berkeley Nuclear Labs, RD/B/N 4643 (1979).
[7] D.S. Kim, M. Bürger, G. Fröhlich and H. Unger, Experimental investigation of hydrodynamic fragmentation of gallium drops in water flows, Proc. International Meeting on Light Water Reactor Severe Accident Evaluation, Cambridge, MA, Aug. 28–Sept. 1, 1983, Vol. 1, 6.4-1.
[8] T.G. Theofanous, M. Saito and T. Efthimiadis, The role of hydrodynamic fragmentation in fuel–coolant interactions, Fourth CSNI Specialist Meeting on Fuel–Coolant Interactions in Nuclear Reactor Safety, Bournemouth, England, April 2–5, 1979, CSNI Report No. 37, Vol. 1, 112, Paper #FC14/P5 (1979).
[9] T.G. Theofanous et al., LWR and HTGR coolant dynamics: The containment of severe accidents, NUREG/CR-3306, U.S. Nuclear Regulatory Commission (July 1983).
[10] S.J. Board and R.W. Hall, Propagation of thermal expansions. Part 2: a theoretical model, Berkeley Nuclear Labs, RD/B/N 3249 (1974).
[11] A. Thayagaraja and D.F. Fletcher, Buoyancy-driven, transient, two-dimensional thermo-hydrodynamics of a melt-water–steam mixture, Computers and Fluids 16 (1988) 59.
[12] W.G. Reinecke and G.D. Waldman, Investigation of water drop disintegration in a region behind strong shock waves, Third Int. Conf. on Rain Erosion and Related Phenomena, Hampshire, UK (1970).
[13] M. Bürger, W. Schawalbe and H. Unger, Application of hydrodynamic and thermal fragmentation models and a steady state thermal detonation model for molten salt-water vapor explosions, Int. Meeting on Thermal Nuclear Reactor Safety, Chicago, Illinois (1982).
[14] P.D. Patel and T.G. Theofanous, Hydrodynamics fragmentation of drops, J. Fluid Mech. 103 (1981) 207–223.
[15] M. Bürger, K. Müller, M. Buck, S.H. Cho, A. Schatz, H. Schins, R. Zeyen and H. Hohmann, Examination of thermal detonation codes and included fragmentation models by means of triggered propagation experiment in a tin/water mixture, Nucl. Engrg. Des. 131 (1991) 61–70.
[16] M. Corradini, Personal communication (1992).